Quasi-one-dimensional particle-in-cell simulation of magnetic nozzles

IEPC-2015-357/ISTS-2015-b-357

Presented at Joint Conference of 30th International Symposium on Space Technology and Science, 34th International Electric Propulsion Conference and 6th Nano-satellite Symposium
Hyogo-Kobe, Japan
July 4–10, 2015

Frans H. Ebersohn*, JP Sheehan† and Alec D. Gallimore‡
University of Michigan, Ann Arbor, MI, 48109, USA

John V. Shebalin §
NASA Johnson Space Center, Houston, TX, 77058, USA

A method for the quasi-one-dimensional simulation of magnetic nozzles is presented and simulations of a magnetic nozzle are performed. The effects of the density variation due to plasma expansion and the magnetic field forces on ion acceleration are investigated. Magnetic field forces acting on the electrons are found to be responsible for the formation of potential structures which accelerate ions. The effects of the plasma density variation alone are found to only weakly affect ion acceleration. Strongly diverging magnetic fields drive more rapid potential drops.

Nomenclature

a = acceleration
B = magnetic field
E = electric field
f = velocity distribution
F = force
J = current density
n = number density
m = particle mass
q = particle charge
r_L = Larmor radius
T_e = electron temperature
v = velocity
$v_\parallel$ = velocity parallel to magnetic field
$v_\perp$ = velocity perpendicular to magnetic field
ϵ_0 = permittivity of free space
ϕ = potential
μ = magnetic moment

*Ph.D. Candidate, Department of Aerospace Engineering, ebersohn@umich.edu
†Assistant Research Scientist, Department of Aerospace Engineering, sheehanj@umich.edu
‡Arthur F. Thurnau Professor, Department of Aerospace Engineering, alec.gallimore@umich.edu
§Exploration Integration and Science Directorate, john.v.shebalin@nasa.gov

I. Introduction

Electrodeless plasma thrusters enable the use of more energy dense plasmas and mitigate some of the lifetime issues of electric propulsion thrusters.[1–3] These devices typically consist of radio-frequency (RF) plasma source and an applied magnetic field known as a magnetic nozzle, shown in Fig. 1, which directs the flow of the plasma. Thrust is generated by the plasma through the pressure forces (P_{int}) on the walls of plasma source and the interaction of the plasma with the magnetic nozzle. Understanding the complex plasmadynamics in the magnetic nozzle is essential to optimizing the performance of electrodeless plasma thrusters.

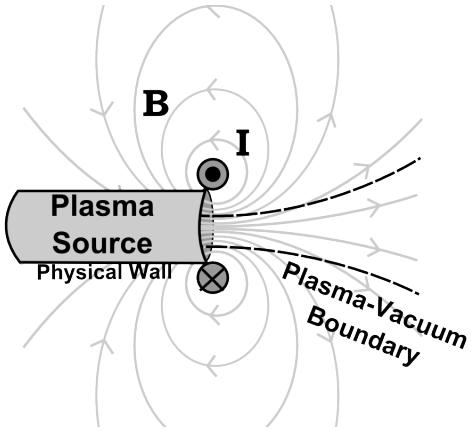

Figure 1: Magnetic nozzle diagram. The magnetic field (**B**) is created by a solenoid with current, **I**.

The physics of magnetic nozzles has been investigated in a number of experiments. The devices tested range from the VAriable Specific Impulse Magnetoplasma Rocket (VASIMR)[4] with very high powers (100's of kW) to the Helicon Double Layer Thruster (HDLT)[3,5] and the CubeSat Ambipolar Thruster (CAT)[6] at low powers(10's -100's of W). The physics which govern ion acceleration in each of these devices is important due to the implications on thruster performance. Both VASIMR and the HDLT have potential drops in the plasma plume which accelerate the ions. The VASIMR experiment[7] showed a long (10000's of Debye lengths) potential drop characteristic of an ambipolar field while the HDLT experiment showed a sharp ($\sim$ 10 Debye lengths)[3,5] potential drop characteristic of a current free double layer. The parameters that govern which type of potential structure forms remains an open question as well as which conditions are best for thruster performance.

VASIMR, HDLT, and CAT operate on the edge of the continuum regime which makes studying the governing physics challenging both with theory and simulation.[8,9] The problem is also inherently multi-scale with the high density plasma source region operating in a regime on the edge of where the continuum assumptions are valid. The density then rapidly drops in the expanding plasma plume, pushing the physics into regimes where continuum assumptions may no longer be valid and in which a kinetic description is necessary. Recent theory and simulations have typically focused on semi-analytical solutions and simplified fluid descriptions when studying magnetic nozzle physics.[10–17] These studies have yielded a great deal of insight on the plasmadynamics, but questions remain which should be addressed from a kinetic perspective. Some of these topics of interest are: the validity of continuum assumptions, the evolution of the energy distribution and its dependence on plasma parameters, the types of ion accelerating potential structures formed in magnetic nozzle experiments, and the effects of instabilities on the plasmadynamics.

Previous kinetic studies of magnetic nozzles have focused on simulations with one-dimensional Particle-in-Cell (PIC) codes.[18,19] Kinetic simulation of magnetic nozzles is difficult because it is an inherently multi-dimensional problem. Simulation with higher dimensions becomes prohibitively expensive for the already computationally taxing problem of simulating a plasma kinetically. The one-dimensional simulations of Meige[18] and Baalrud[19] investigated the conditions which lead to the formation of a double layer in a configuration similar to the HDLT.[3] The expansion process was mimicked by including a loss frequency for

removing particles from the simulation over a portion of the domain. Formation of double layers was found to be dependent on this loss frequency, with double layers appearing for sufficiently high loss frequencies. This implies that double layers form when the plasma rapidly expands. These simulations also showed the formation of an accelerated ion beam due to this potential structure. Meige and Baalrud both acknowledge the limitations of this model and suggest future work which includes the effects of the magnetic field and better captures the expansion. The work presented in this paper further investigates this problem by neglecting the loss frequency and modeling the two dimensional effects of the magnetic nozzle on the plasma by including the effects of the density variation due to the plasma expansion and magnetic field forces using a new quasi-1D (Q1D) method. This work attempts to address the need for a more robust simulation which includes two-dimensional effects without increasing the computational cost prohibitively.

Section II of this paper will give a more in-depth background on magnetic nozzle physics while Section III presents the new quasi-one-dimensional model. Section IV discusses the code used and simulation parameters. Results are presented and discussed in Sections V and VI respectively with Section VII concluding the paper.

II. Background

Magnetic nozzles are strong guiding magnetic fields used to direct and accelerate the flow of a plasma. Among the important physical processes are: 1) the mechanisms by which energy is exchanged in the plasma leading to ion acceleration, 2) the interactions between the plasma and the device which generate thrust, and 3) the detachment of the plasma from the initially confining magnetic field lines. This work focuses on improving the understanding of the energy exchange mechanisms which govern ion acceleration in order to give insight on better designing magnetic nozzle thrusters. Ions can be accelerated in the magnetic nozzle through interaction with induced electric fields or the applied magnetic field, each of which is discussed below.

A. Induced Electric Fields Effects

Plasma expansion from a quasi-neutral region can lead to the formation of potential structures in the plasma. The rapid thermal expansion of the light electrons compared to the slow expansion of the massive ions can lead to the formation of an electric field which strives to maintain quasi-neutrality in the plasma, as shown in Fig. 2. This electric field accelerates the ions resulting directed ion kinetic energy along the electric field. The potential structure which develops has shown characteristics of a double layer (a rapid drop in potential over a few Debye lengths)[3] and an ambipolar field (gradual drop in potential over 10000's of Debye lengths).[7] Another key difference between these mechanisms is seen in the electron temperature, which varies only slightly over the double layer, but shows large gradients in ambipolar fields.[20] The conditions which lead to the formation of these potential structures remains an open question, as well as their effectiveness in producing thrust.[21] This simplified discussion has neglected collisions, which may also play an important role in the formation of these potential structures.

B. Magnetic Field Effects

Particles in a magnetic field are considered to be magnetized when the magnetic field is strong enough that the particles follow small orbits around the field line. Magnetization requires that the particle orbit radius, known as the Larmor radius ($r_L = mv_\perp/qB$), is small compared to a characteristic dimension. In this equation $v_\perp$ is the velocity perpendicular to the magnetic field, B is the magnetic field, m is the particle mass, and q is the particle charge. Electrons are magnetized both in the source and near plume of magnetic nozzle thrusters. The ions however may not be magnetized due to their large mass which increases the ion Larmor radius. This leads to some magnetic nozzle thrusters having magnetized ions, while others do not.

The orbits of magnetized particles in a magnetic nozzle can be imagined as small current loops. These current loops feel a force similar to the magnetic dipole force shown in Eq. (1).[22] In this equation, $\mu = \frac{mv_\perp}{2|B|}$ is the magnetic moment.

$$\mathbf{F} = \nabla \left(\mu \cdot \mathbf{B} \right) \tag{1}$$

This force acts along a magnetic field line, accelerating magnetized particles from strong magnetic field regions into weak magnetic field regions. All magnetized particles are affected by this force which can

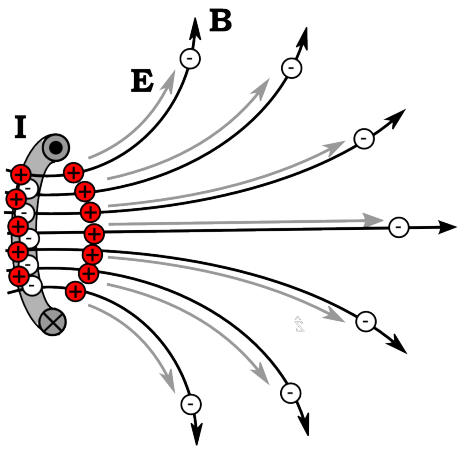

Figure 2: Electric field generated in a magnetic nozzle by electron thermal expansion

accelerate both the ions and the electrons. The magnetic field does no work, but only redirects the velocity perpendicular to the magnetic field ($v_\perp$) to a direction parallel to the magnetic field ($v_\parallel$). By this mechanism perpendicular kinetic energy of a particle is converted to directed kinetic energy along the magnetic field line. This force is a simplification of the Lorentz force valid only for magnetized particles.

C. Coupled Electric and Magnetic Field Effects

The effects of the magnetic and electric field can also couple to one another leading to further acceleration of the ions.[23,24] As mentioned previously, electrons rapidly expand away from the plasma source due to their thermal velocity. This expansion leads to the formation of a potential structure in the plasma. Without the magnetic field present, the electron thermal expansion and the potential reach an equilibrium condition where the thermal expansion and the potential structure balance one another. The addition of the magnetic field effects in a diverging magnetic nozzle leads to force which drives the expanding electrons outward, away from the high magnetic field region in the the same direction as the expansion. The potential structure must now balance both the thermal expansion of the electrons and the magnetic field forces on the electrons. A strong electric field, stronger than without the magnetic field effects, develops due to this magnetic field driven electron expansion. This stronger electric field leads to a larger potential drop and more ion acceleration. The ion acceleration is thereby affected by the magnetic field through the electrons, even if the ions are not magnetized themselves.

D. Role of Kinetic Simulations

Kinetic simulations should be used to study these ion acceleration mechanisms in the most general way because the forces which drive these mechanisms arise from a particle perspective and not a continuum perspective. Furthermore, the devices of interest in this research (VASIMR, HDLT, CAT) operate in regimes where continuum assumptions may no longer be valid. This motivates the use of particle based codes to generally describe the physics and determine the validity of continuum assumptions to describe these thrusters.

III. Methodology

Electrostatic PIC codes treat the plasma as a collection of particles or macroparticles while solving for macroscopic quantities and fields on a grid.[25–27] The particle motion is governed by the Lorentz force and the electric field is calculated by solving Poisson's equation using charge densities collected on the grid. A

quasi-one-dimensional PIC solver (QPIC) was developed as an extension to one-dimensional PIC solvers to study magnetic nozzles by including two-dimensional effects.

QPIC resolves the centerline axis ($\hat{z}$) of the magnetic nozzle spatially and includes three velocity dimensions. An example of the simulation domain is shown in Fig. 3. The domain includes a heating region in which the magnetic field is constant and expansion region in which the magnetic field decreases. Particle-neutral collisions are modeled using the null collision algorithm.[28] Electron-neutral elastic, inelastic, and ionization collisions were included as well as ion-neutral elastic and charge exchange collisions. Collision cross-section data was used in tabulated form based on literature.[29–31] The methods used for incorporating two-dimensional effects included variation of the cross sectional area of the one-dimensional domain and the magnetic field forces.

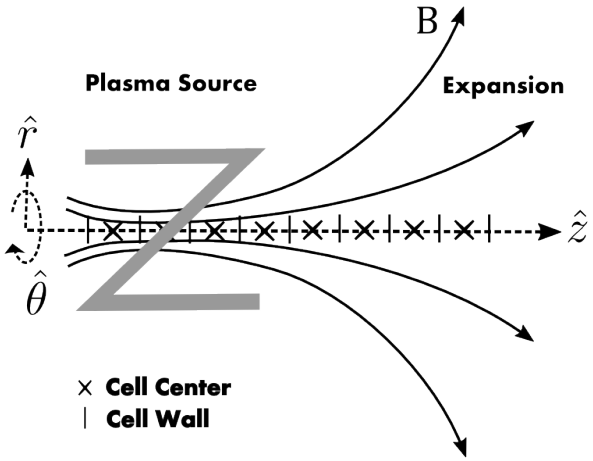

Figure 3: Quasi-1D particle simulation domain. The centerline axis is resolved as shown by the cells along this field line.

A. Heating Region

The particles were heated in the heating region according to the mechanism described by Meige.[18] The perpendicular electric field is varied according to Eq.(2) below in which E_y is the electric field in the $\hat{y}$-direction and J_y is the current density in the $\hat{y}$-direction. The $\hat{y}$-direction is in the $\hat{r} - \hat{\theta}$ plane which is perpendicular to the axial direction($\hat{z}$).

$$J_{y,tot} = \epsilon_0 \frac{\partial E_y}{\partial t} + J_{y,conv} \tag{2}$$

The plasma convective current ($J_{y,conv}$) is found by summing over the particles (both ions and electrons) in the heating zone, while the total applied current is varied as desired. For the simulations in this paper the applied current was of the form $J_{y,tot} = J_0 sin(\omega t)$. The frequency ($\omega = 2\pi \times 10^7\ rad/s$) was chosen to reflect typical radio-frequency (RF) discharges and the current amplitude ($J_0 = 100\ A/m^2$) chosen so that the densities in the source region were similar to experiments. The varying electric field resulting from this method heats the electrons which can then collide with the neutral background to produce additional ions and electrons.

B. Cross-sectional area variation

The density variation due to the plasma expansion was captured by varying the cross-sectional area of the domain. The cross-section was found by assuming that the particles follow the magnetic field lines. This bounds the plasma plume within a particular magnetic flux surface as shown in Fig. 4. The cross-section

of this flux surface can be approximated by using Gauss' Law of Magnetism and assuming that the radial magnetic field (B_r) contributes negligibly to the total flux leaving the tube($B_r << B_z$). This assumption leads to the expression shown in Eq. (3) while relates the on-axis magnetic field (B_z) to the cross-sectional area of the flux-tube. Knowing the axial magnetic field profile and the inlet area (A_{in}) determines the area of the flux tube throughout the domain. This area is then used in the calculation of plasma densities.

$$A = \frac{B_{z,in}}{B_z} A_{in} \tag{3}$$

The cross-sectional area variation models the effects of the magnetic field compression and expansion on the plasma density. The area variation couples to the other governing equations through the calculation of the density of the particles, which in turn affects the solution of Poisson's equation.

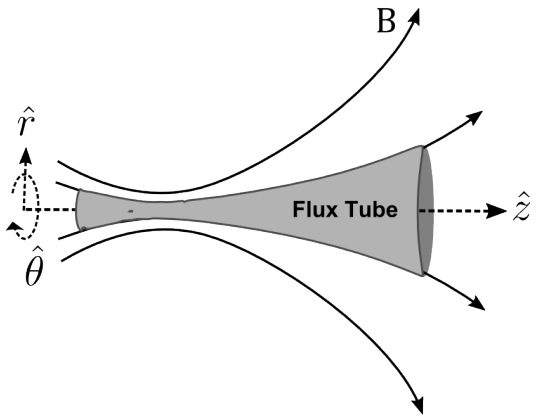

Figure 4: Flux-tube cross sectional area variation.

C. Magnetic Field Force

The effects of magnetic field forces on the plasma in a magnetic nozzle must also be included to more completely study magnetic nozzle physics. A force along the magnetic field line can be derived from the magnetic field contribution to the Lorentz force in cylindrical coordinates shown in Eq (4).

$$\frac{\partial \mathbf{v}}{\partial t} = \frac{q}{m}(\mathbf{v} \times \mathbf{B}) + \mathbf{a}_{coord} \tag{4}$$

In the above equation $\mathbf{a}_{coord}$, corresponds to the acceleration due to inertial effects which come as a results of the cylindrical coordinate system chosen, $\mathbf{v}$ is the velocity of the particle, and q is the charge of the particle. The inertial acceleration is shown in Eq. (5).

$$\mathbf{a}_{coord} = \frac{v_\theta^2}{r_L}\hat{r} - \frac{v_\theta v_r}{r_L}\hat{\theta}. \tag{5}$$

The Lorentz force can be simplified by imagining the magnetized particles as small current loops orbiting around a magnetic field line (the centerline magnetic field line in this case) with radii equal to their Larmor radii(r_L).[32] Gauss' Law of Magnetism in cylindrical coordinates is then used to simplify these equations by assuming that the axial magnetic field does not vary over the particle orbit. This leads to an expression for the radial magnetic field a particle experiences while orbiting a particular magnetic field line:

$$B_r = -\frac{r_L}{2}\frac{\partial B_z}{\partial z} \tag{6}$$

In this equation r_L is the Larmor radius defined previously. Substitution of the radial magnetic field into the Lorentz force leads to a significant simplification of the equations to the forms shown in Eq. (7)-(9).

$$\frac{\partial v_z}{\partial t} = -\frac{1}{2B_z}\frac{\partial B_z}{\partial z}v_\theta^2 \tag{7}$$

$$\frac{\partial v_\theta}{\partial t} = \frac{1}{2B_z}\frac{\partial B_z}{\partial z}v_\theta v_z \tag{8}$$

$$\frac{\partial v_r}{\partial t} = 0 \tag{9}$$

The coordinate system forces are canceled by the magnetic field forces which bind the particles to the magnetic field line. This cancellation occurs due to the inherent assumption of magnetization. The only forces that remain are a force which acts along the magnetic field line ($\hat{z}$) similar to the dipole force and a corresponding force in the azimuthal ($\hat{\theta}$) direction which conserves energy.

In this derivation it has been implicitly assumed that the particles are in a frame of reference along a magnetic field line. The azimuthal velocity was used to define the orbit, but more generally this is the velocity perpendicular to the magnetic field ($v_\perp$). Equations 10 and 11 show the forces in the frame of reference of the magnetic field with s defining the direction along the magnetic field.

$$\frac{\partial v_\parallel}{\partial t} = -\frac{1}{2B}\frac{\partial B}{\partial s}v_\perp^2 \tag{10}$$

$$\frac{\partial v_\perp}{\partial t} = \frac{1}{2B}\frac{\partial B}{\partial s}v_\perp v_\parallel \tag{11}$$

IV. Simulation Parameters

Simulation parameters are chosen to compare with previous one-dimensional simulations by Meige[18] and Baalrud[19] in regimes of operation similar to the HDLT.[3] The goal of these simulations is to further study this problem by including the two-dimensional effects described in the previous section without assuming a loss frequency for the particles. The simulation domain consists of a heating region from $x = (0.0, 0.05)\ m$ which is followed by an expansion region from $x = (0.05, 0.1)\ m$. The left boundary is a floating collector while the right boundary is grounded. The simulation parameters are shown in Table 1.

Table 1: Parameters for magnetic nozzle simulations

Parameter	Value
Length	10 cm
Grid Cells	250
Time Step	$5 \times 10^{11}\ s$
Total Time	25 μs
Heating Current	100 A/m^2
Heating Frequency	$1 \times 10^7\ Hz$
Macroparticle Weight	2×10^8 Particles/Macroparticle
Neutral Pressure	1.23 $mTorr$
Neutral Temperature	293 K
Gas	Argon
Magnetic Field (B_0)	300 G

The effects of the cross-sectional area variation and the magnetic field forces on the simulation results were investigated individually and together. The effects of ion magnetization were also investigated by including and neglecting the magnetic field forces on the ions. The applied magnetic field magnitude ($B_0 = 300\ Gauss$) is chosen to represent something similar to that seen in the experiments.[3,33] The magnetic field is constant in the heating region and then decreases in the expansion region. The magnetic field profile along the axis is chosen to take a form similar to that for the magnetic field along the centerline of a current loop.[19] Equation 12 shows this relation.

$$B_z = \frac{B_0}{\left(1 + \frac{(z-0.05)^2}{C^2}\right)^{3/2}} \tag{12}$$

The constant C in this equation is varied to change the how rapidly the magnetic field diverges. Figure 5 shows the magnetic field topologies tested in these simulations. These cases will be referenced throughout the results section. Case 1 in all simulations corresponds to a simulation in which there is no magnetic field expansion ($B(z) = B_0$) while Case 4 is the strongest expansion. The values for C for Cases 2-4 are 0.04, 0.02, and 0.01 respectively.

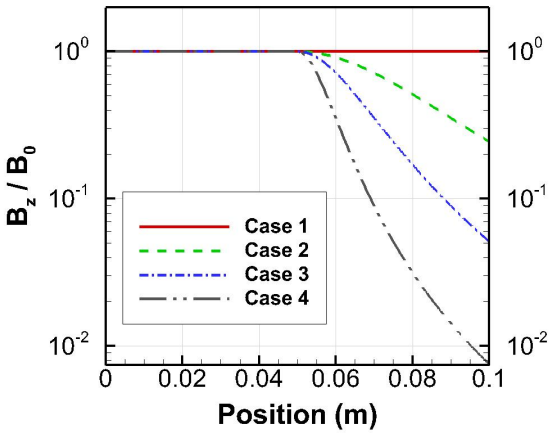

Figure 5: Magnetic field topologies used in simulations

V. Results

Four sets of simulations were performed using the parameters described in the previous section to investigate how the two-dimensional effects included by the quasi-1D formulation affect the one-dimensional results. The first set investigated the effects of the cross-sectional area on density only while the second set investigated the magnetic field force only. The third set included both effects together. The fourth set includes the effects of the cross-sectional area variation and only includes magnetic field forces on the electrons. This final set corresponds to a condition in which the ions are not magnetized. The results shown for all simulation were averaged over the last heating cycle. A discussion of Case 1 is given below as a reference for all the other cases and across the simulation sets. Case 1 is a truly one-dimensional simulation and is the same in each of the sets. A discussion of Case 4 for the full simulation without ion magnetic field forces is also given to analyze the particle kinetics.

A. One-Dimensional Simulation (Case 1)

Case 1 in all simulation sets corresponds to the case where the magnetic field is constant resulting in no two-dimensional effects in the quasi-1D model. This case is the baseline case which serves as a one-dimension point of reference for each of the simulation sets and across the different sets. Simulation parameters for this case are similar to the case presented by Meige for a discharge with zero loss frequency and a background neutral pressure of $P_{neut} = 1\ mTorr$.[18] The simulation results of this paper and those of Meige show similar behavior, although they are not identical due to the slightly different neutral pressure used, cross-section data, and the difference in the heating scheme. In our simulations the ion current is also included in calculating the plasma conduction current (J_{cond}).

This case (see Case 1 in Fig. 6-8) shows the formation of a sheath at the left floating boundary as well as a sheath at the right grounded boundary. The density is nearly uniform through the rest of the domain. A source sheath is not seen at the edge of the heating region because charged particles are created

not only in this region, but throughout the domain due to electron-neutral collisions. This is an important phenomenon which effectively stretches the source region beyond where heating occurs and eliminates the source sheath. The creation of particles outside the heating region inhibits the formation of the potential structures mentioned in Section II which may occur due to the rapid thermal expansion of electrons from a finite source.

The electron and ion axial velocity distributions (f) as well as the electron temperature (T_e) are shown in Fig. 6a - 6c for the final time-step. These are not time-averaged quantities, but only from a single time step. The directional electron temperature is calculated by finding the average directional kinetic energy of particles in a cell (KE_{avg}) and using the following equation: $KE_{avg} = \frac{1}{2}k_b T_e$. The total temperature is found by a similar equation using 3/2 as the constant instead of 1/2 and finding the total kinetic energy of the particle.

The electron temperature in these simulations is found to be around 4 eV and increases near the edges of the domain. The temperature in the $\hat{y}$-direction is slightly higher due to the heating in this direction. The electron axial velocity distribution stays nearly the same through the domain with slight variations with the electron temperature. The ion axial velocity distribution shows some acceleration of the ions through the pre-sheath.

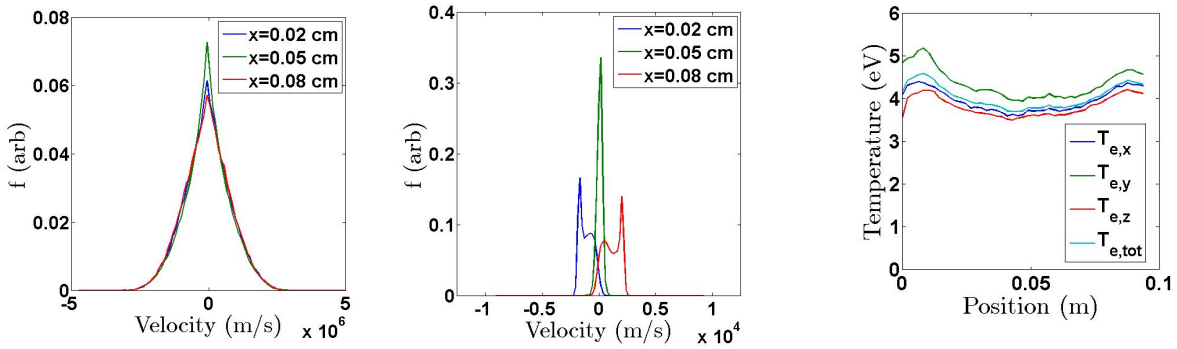

(a) Electron axial velocity distribution. (b) Ion axial velocity distribution. (c) Electron temperatures spatially.

Figure 6: Case 1 Results

B. Density Effects

The first set of simulations only included the effects of the cross-sectional area variation on the jet expansion. These simulations capture the decreases in density that occur due to the plasma expanding along the magnetic field lines. The results from these simulations are shown in Fig. 7a-7d. Both the electron (a) and the argon (b) densities decrease as the plasma expands. As expected, a more pronounced expansion occurs for the more strongly diverging magnetic field. The plasma potential (c) is not significantly affected by the expansion region. A slight decrease in the overall potential is seen and no rapid potential drops similar to a double layer are present at the beginning of the expansion. Case 4 shows what looks like an extended sheath region which is likely due to the decease in density and the resulting increase in Debye length. The ion mean velocities also do not change significantly, with Case 4 showing a slight acceleration due to the extended sheath region.

These results indicate that the effects of the density decrease resulting from the plasma expansion does not by itself result in the formation of sharp, ion-accelerating potential structures. A possible reason for this is that the variation of density alone does not have a mechanism which would drive the plasma to establish these structures. As illustrated in Case 1, no source sheath is established at the edge of the heating region because the collisions of the electrons with the background neutrals throughout the domain generate plasma outside the heating region. These collisions effectively stretch the source region beyond where the plasma is heated into the expansion region. The decrease of the electron and argon densities in the expansion region does not affect this source stretching behavior because the collisionality of the ions and electrons with the background neutrals is not a function of the ion or electron densities. The collision frequency of the particles

is given by $\nu = n_{neut}\sigma v_{rel}$ in which n_{neut} is the background density, σ is the collision cross-section, and v_{rel} is the relative velocity of the particles. The neutral density is constant in the domain and neither the collision cross-section or the relative velocity are a function of the plasma density. Future simulations will investigate varying the neutral background pressure and neutral density, which will affect the region over which plasma is generated and may result in the formation of source sheaths.

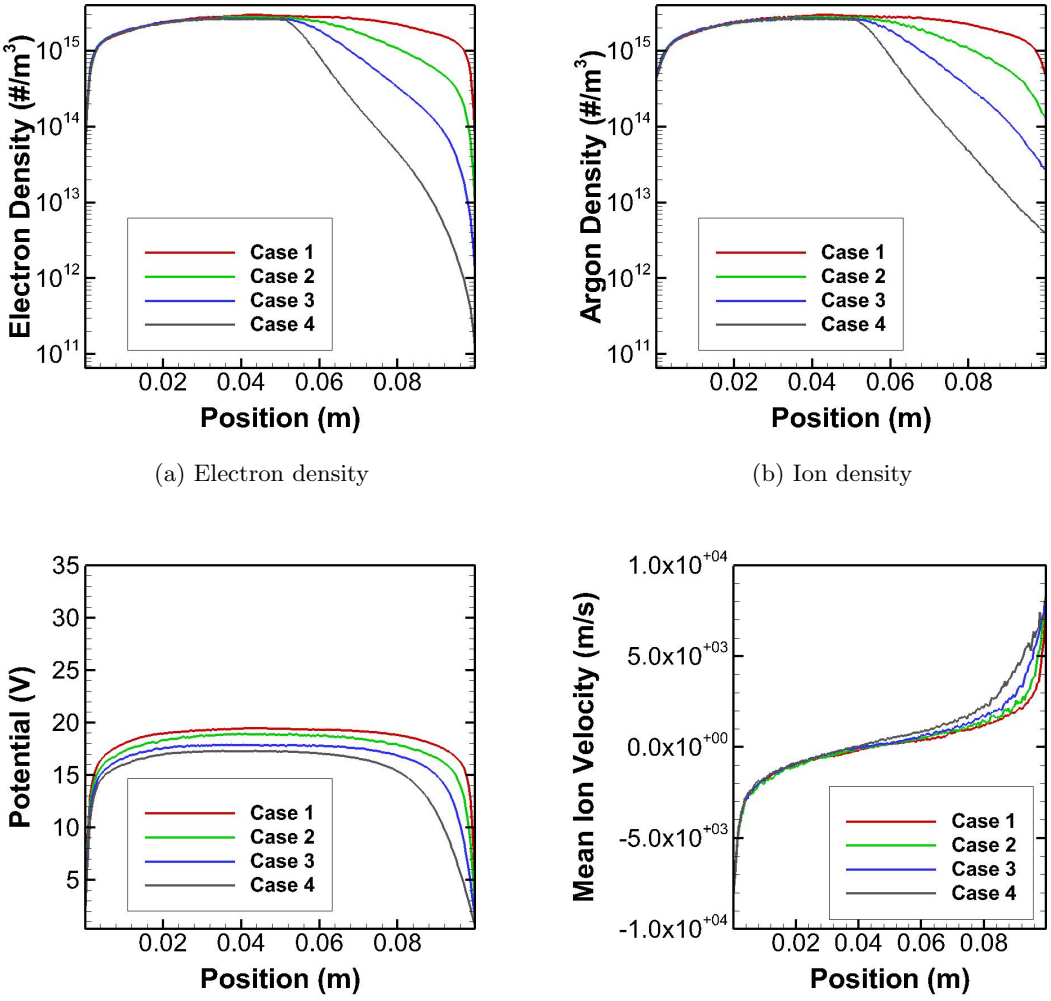

(a) Electron density

(b) Ion density

(c) Potential

(d) Mean ion velocity

Figure 7: Density effect simulations

C. Magnetic Field Forces

The next set of simulations included the effects of the magnetic field forces. Both ions and electrons are assumed to be magnetized and are affected by the magnetic field forces. The results of these simulations are shown in Fig. 8a - 8d. Both the electron (a) and ion (b) number densities show a slight decrease in the diverging magnetic field cases. The stronger the divergence, the more the decrease in density. The plasma potential (c) was greatly affected by the magnetic field forces. A large drop in potential is seen as the plasma diverges. The magnitude of this potential drop increased as the magnetic field divergence increased. The length over which the potential decreases is large and future simulations will investigate the effect of the boundary location on the potential structure. The mean ion velocity (d) shows that the ions are accelerated with more significant ion acceleration seen for the rapidly diverging magnetic field. This

increased acceleration is due to the lower value of the final magnetic field in the sharply diverging simulations. Ion acceleration does not continue for the whole expansion due to the effects of ion-neutral collisions.

The effects of the magnetic field force on the plasma lead to the formation of a potential structure which accelerates the ions. The magnetic field force rapidly accelerates the electrons outwards ahead of the ions. The magnetized ions are also accelerated by the magnetic field forces, but the magnitude of this force is much less for the ions. This is due to the fact that the magnetic field forces are a function of the perpendicular velocity ($v_\perp$) which is much smaller for the ions. Therefore, the ions lag behind the electrons, leading to the formation of the potential structure that also accelerates the ions. This hypothesis will be further investigated in the final set of simulations which remove the magnetic force effects on the ions while still including the magnetic field forces on the electrons.

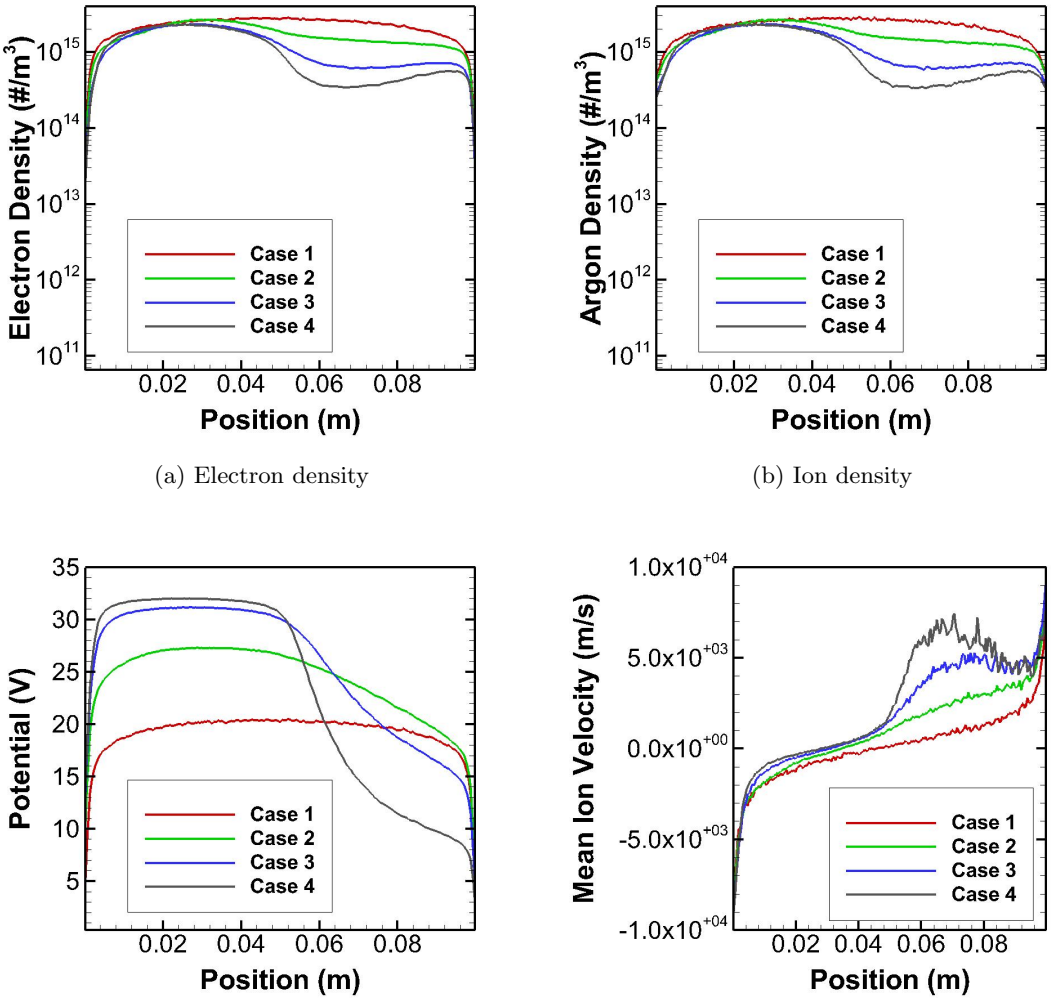

(a) Electron density

(b) Ion density

(c) Potential

(d) Mean ion velocity

Figure 8: Magnetic field force simulations

D. Full Simulation

Test cases with both the area variation and the magnetic field force were simulated. The results of these simulations are shown in Fig. 9a-9d. Electron (a) and ion (b) densities show the characteristics of both previous simulation sets with a drop in density due to a combination of the cross-sectional area variation and magnetic field force acceleration. The potential (c) also shows characteristics of both previous test cases

with a rapid drop in potential seen for the rapidly diverging field cases and a lengthened sheath. The ions velocities (d) also increase as the plume expands more rapidly. The acceleration of the ions does not continue through the entire potential drop due to a balance between the accelerating potential and the collisions with the neutral background.

These simulations show the characteristics of both the previous simulations, but are most similar to the magnetic field effect simulations. A sharp density drop is present as well as electron-driven potential structures which accelerate the ions. Incorporation of both these effects provides the most complete picture.

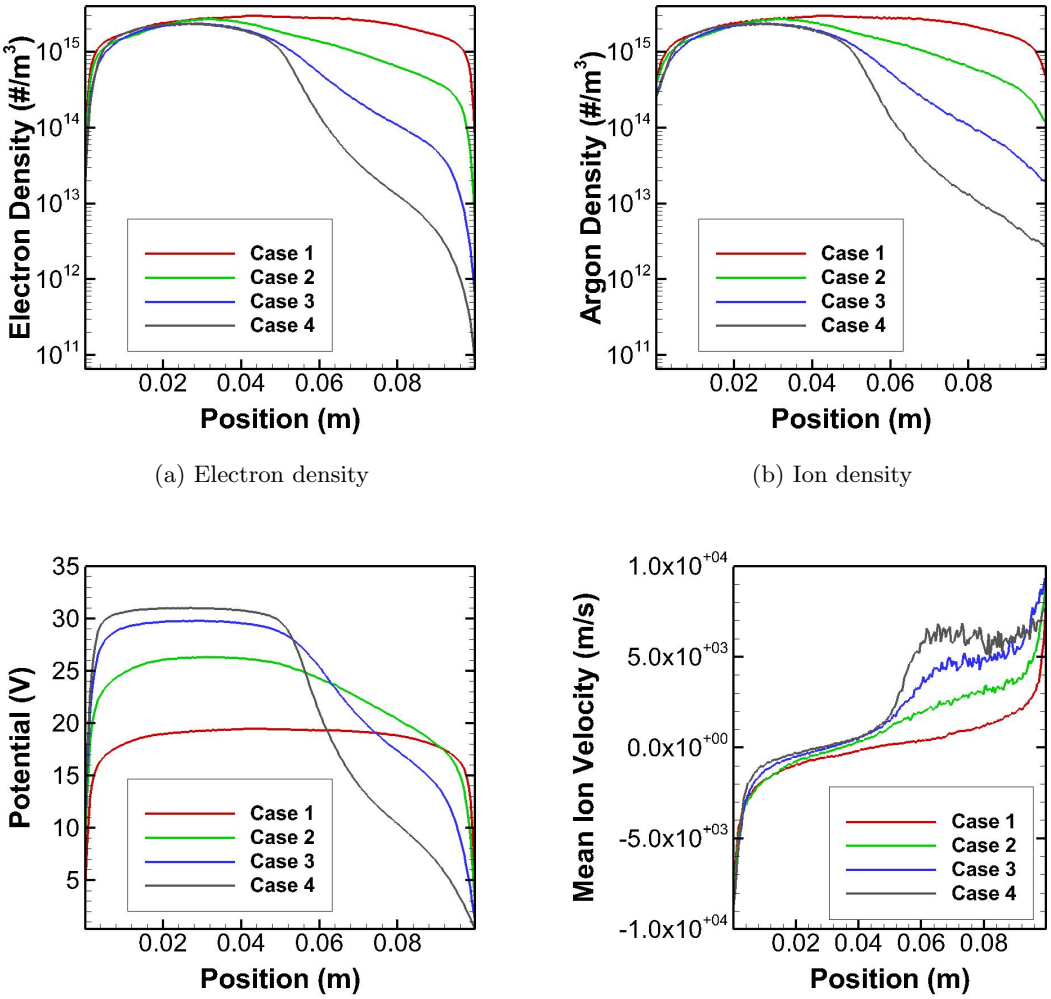

(a) Electron density

(b) Ion density

(c) Potential

(d) Mean ion velocity

Figure 9: Full simulations with magnetic field forces and area variation.

E. Full Simulation with Demagnetized Ions

Finally simulations were performed with the effects of the magnetic field forces on the ions removed while including the cross-sectional area variation effects and the electron magnetic field forces. This simulates conditions in which the ions would be demagnetized, but still on average follow the magnetic field lines. The results of these simulations is shown in Fig. 10a-10d. These plots show that the results are very similar to the results of the full simulation which includes the ion magnetic field forces. This suggests that the effects of the magnetic field forces on the ions is negligible for these conditions in comparison to the other forces. Therefore, these simulation results validate the arguments that the ion acceleration is not caused directly by

the magnetic field forces on the ions. The ions acceleration is instead caused by potential structure which establishes as a result of the magnetic field forces on the electrons.

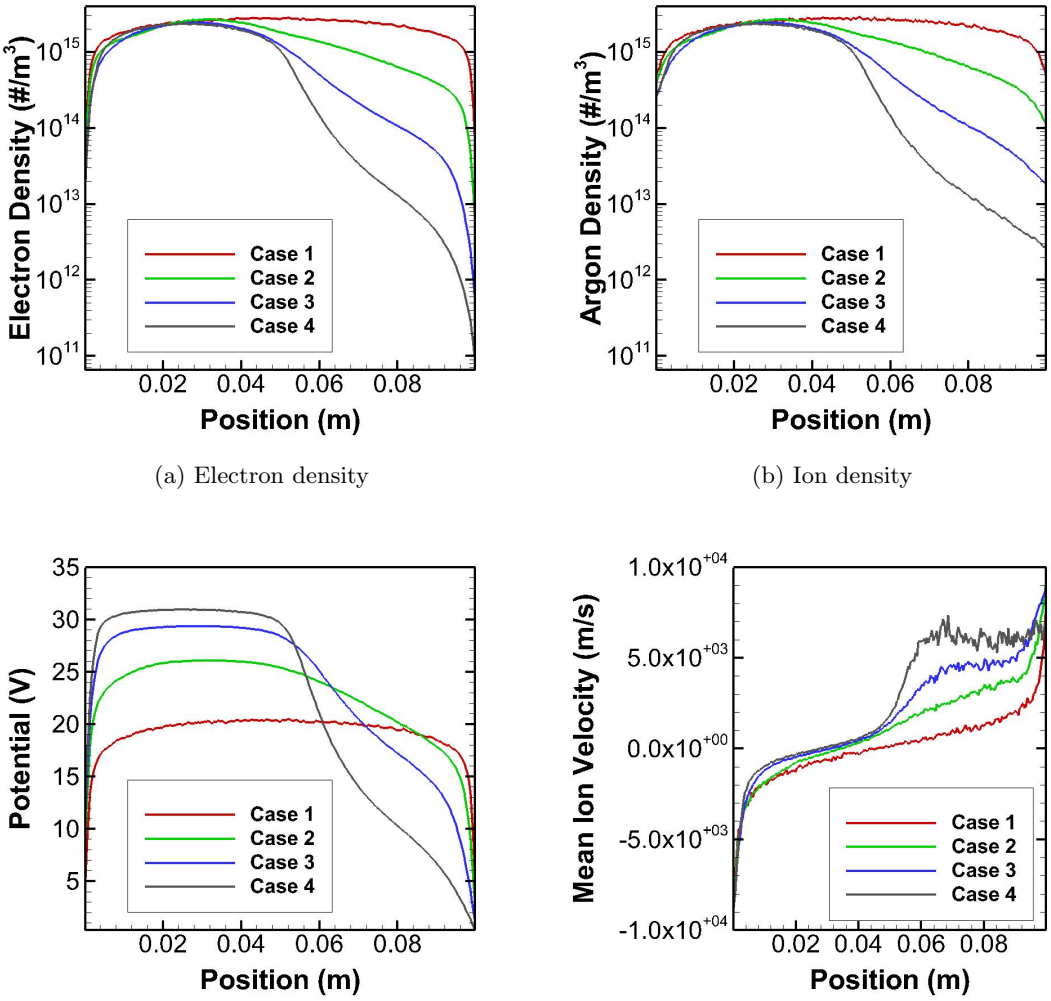

(a) Electron density

(b) Ion density

(c) Potential

(d) Mean ion velocity

Figure 10: Full simulations with magnetic field forces on the electrons and cross-sectional area variation.

F. Case 4

Further analysis of Case 4 of the full simulations ignoring ion magnetic field forces was performed study the kinetic effects on the plasma. The electron and ion axial velocity distributions as well as the electron temperature are shown in Fig. 11a - 11c. The electron temperature reaches a local minimum in the heating region with maximums at the edges of the heating region. This is much different from the constant temperature seen in Case 1. As the electrons expand they cool and the temperature decreases. The electron velocity distribution varies spatially as the electron temperature varies and no beam or mean velocity of electrons is seen. The electrons maintain a distribution that is nearly Maxwellian.

The ion velocity distribution shows the development of a sharp peak corresponding to the accelerated beam of ions created as the plasma expands. Charge-exchange collisions create the broad velocity distribution at lower energies. The ions are not accelerated indefinitely due to the collisions with the neutral background. The beam velocity reached occurs as a balance between the accelerating potential and the ion-neutral collisions.

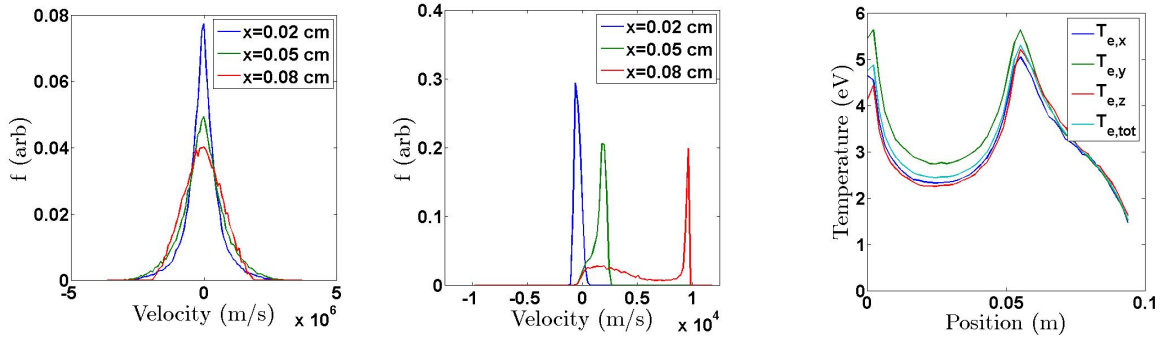

(a) Electron axial velocity distribution. (b) Ion axial velocity distribution. (c) Electron temperature spatially.

Figure 11: Case 4 results with no ion magnetization, magnetic forces on electrons, and cross-sectional area variation.

VI. Discussion

Previous simulations have investigated the ion accelerating potential structures by using one-dimensional PIC codes and a loss frequency in the expansion region of the domain.[18,19] These simulations showed similar results to those found in this paper, but with a very different model to examine the expansion region. The loss frequency method is implemented in a way similar to a collision frequency and removes particles from the domain to mimic the density decrease as the plasma expands. These simulations showed that a sharp drop in potential similar to a double layer occurs when the loss frequency of particles is large enough. This double layer then accelerates the ions.

Based on these previous simulation results, it was hypothesized that including the effects of the density variation in the plasma expansion using the quasi-1D model of this paper would produce similar results. However, the results of the previous section suggest that the density variation due to the expansion does not result in the formation of any ion accelerating potential structures and that instead these structures form due to the magnetic field forces which act on the electrons. The magnetic field forces accelerate both the electrons and ions along the field line. The high energy electrons are more greatly affected by the accelerating magnetic field forces which are a function of $v_\perp^2$. The ions have much lower perpendicular velocity which results in a much weaker accelerating force. Rapid acceleration of the electrons relative to the ions leads to the formation of a potential structure that accelerates the ions to keep up with the electrons. Ion acceleration is governed by the potential structure established by the magnetic field force driven electron acceleration. This is further confirmed by the simulations which remove the effects of the magnetic field force on the ions which still show acceleration of the ions due to the formation of a potential structure.

These results suggest that the effects of the density on the expansion alone is not sufficient to establish these potential structures, which may seem contrary to the previous results in literature. This discrepancy can be explained using discussion from these papers. As pointed out by Baalrud, the loss frequency method has an inherent bias for removing slow particles from the domain more frequently.[19] Slow particles are in the domain longer, so there is a higher probability that they are removed. This may result in a higher than expected ratio of high energy particles to low energy particles. Furthermore, the ions are much slower than the electrons, implying that on average the slow ions are more likely to be removed than the fast electrons leading to a higher density of electrons than expected. The higher ratio of energetic, negatively charged particles may result in the formation of a potential structure which accelerates the slow, positively charged ions. A possible way to test this theory would be to add weighting factor to the loss frequency.

VII. Conclusion

Methods for the incorporation of two-dimensional effects in a one-dimensional magnetic nozzle simulation were presented. These methods were used to study the ion acceleration in a magnetic nozzle and it was found that magnetic field effects lead to electron-driven potential structures which accelerate the ions. The effect of plasma density variation due to the nozzle expansion are found to be secondary to the effects of the magnetic field forces. Future simulations will investigate these physics in additional magnetic nozzle experiments such as VASIMR and CAT. The effects of the neutral pressures will also be studied.

Acknowledgments

This research is funded by a NASA Office of Chief Technologist Space Technology Research Fellowship. Simulations were performed on the NASA Pleiades Supercomputer. Thank you to Dr. Kentaro Hara and Dr. Alec Thomas for their guidance and suggestions with validation simulations. The authors thank the members of PEPL for their insightful discussions concerning this research.

References

[1]Dan M Goebel and Ira Katz. *Fundamentals of electric propulsion: ion and Hall thrusters*, volume 1. John Wiley & Sons, 2008.

[2]R.G. Jahn and W. von Jaskowsky. *Physics of Electric Propulsion*, volume 288. McGraw-Hill, New York, 1968.

[3]C Charles. Plasmas for spacecraft propulsion. *Journal of Physics D: Applied Physics*, 42(16):163001, 2009.

[4]F.R. Chang-Diaz. The vasimr rocket. *Scientific American*, 283(5):90–97, 2000.

[5]C Charles, RW Boswell, and MA Lieberman. Xenon ion beam characterization in a helicon double layer thruster. *Applied physics letters*, 89(26):261503–261503, 2006.

[6]JP Sheehan, T Collard, Benjamin W Longmier, and I Goglio. New low-power plasma thruster for nanosatellites. AIAA-2014-3914. 50th AIAA/ASME/SAE/ASEE Joint Propulsion Conference, 2014.

[7]B.W. Longmier, E.A. Bering, M.D. Carter, L.D. Cassady, W.J. Chancery, F.R.C. Díaz, T.W. Glover, N. Hershkowitz, A.V. Ilin, G.E. McCaskill, et al. Ambipolar ion acceleration in an expanding magnetic nozzle. *Plasma Sources Science and Technology*, 20:015007, 2011.

[8]F. Ebersohn, S.S. Sharath, D. Staack, J. Shebalin, B. Longmier, and C. Olsen. Magnetic nozzle plasma plume: Review of crucial physical phenomena. AIAA-2012-4274, Atlanta, GA, July 2012. 47th AIAA/ASME/SAE/ASEE Joint Propulsion Conference.

[9]J.M. Little, A.S. Rubin, and E.Y. Choueiri. Similarity parameter evolution within a magnetic nozzle with applications to laboratory plasmas. IEPC-2011-229, Wiesbaden, Germany, September 2011. 30th International Electric Propulsion Conference.

[10]E. Ahedo and M. Merino. Preliminary assessment of detachment in a plasma thruster magnetic nozzle. AIAA-2010-6613. 45th AIAA/ASME/SAE/ASEE Joint Propulsion Conference, July 2010.

[11]E. Ahedo and M. Merino. Two-dimensional supersonic plasma acceleration in a magnetic nozzle. *Physics of Plasmas*, 17:073501, 2010.

[12]E. Ahedo and M. Merino. On plasma detachment in propulsive magnetic nozzles. *Physics of Plasmas*, 18:053504, 2011.

[13]Merino M. and Ahedo E. Magnetic nozzle far-field simulations. AIAA-2012-3843. 46th AIAA/ASME/SAE/ASEE Joint Propulsion Conference, July 2012.

[14]M. Merino and E. Ahedo. Plasma detachment mechanisms in a magnetic nozzle. AIAA-2011-5999. 46th AIAA/ASME/SAE/ASEE Joint Propulsion Conference, July 2011.

[15]Justin M Little and Edgar Y Choueiri. Thrust and efficiency model for electron-driven magnetic nozzles. *Physics of Plasmas (1994-present)*, 20(10):103501, 2013.

[16]J. Navarro, M. Merino, and E. Ahedo. A fluiddynamic performance model of a helicon thruster. AIAA-2012-3955, Atlanta, GA, July 2012.

[17]J. Navarro, M. Merino, and E. Ahedo. Two-fluid and pic-fluid code comparison of the plasma plume in a magnetic nozzle. AIAA-2012-3840, Atlanta, GA, July 2012.

[18]Albert Meige, Rod W Boswell, Christine Charles, and Miles M Turner. One-dimensional particle-in-cell simulation of a current-free double layer in an expanding plasma. *Physics of plasmas*, 12:052317, 2005.

[19]SD Baalrud, T Lafleur, RW Boswell, and C Charles. Particle-in-cell simulations of a current-free double layer. *Physics of Plasmas (1994-present)*, 18(6):063502, 2011.

[20]JP Sheehan, BW Longmier, EA Bering, CS Olsen, JP Squire, MG Ballenger, MD Carter, LD Cassady, FR Chang Díaz, TW Glover, et al. Temperature gradients due to adiabatic plasma expansion in a magnetic nozzle. *Plasma Sources Science and Technology*, 23(4):045014, 2014.

[21]A. Fruchtman, K. Takahashi, C. Charles, and RW Boswell. A magnetic nozzle calculation of the force on a plasma. *Physics of Plasmas*, 19:033507, 2012.

[22]J.D. Jackson. *Classical electrodynamics*. Wiley, 1999.

[23]J.C. Sercel. Simple model of plasma acceleration in a magnetic nozzle. In *AIAA, DGLR, and JSASS, 21st International Electric Propulsion Conference*, volume 1, 1990.

[24]H.G. Kosmahl. Three-dimensional plasma acceleration through axissymmetric divergine magnetic fields based on dipole moment approximation. Technical report, National Aeronautics and Space Administration,Lewis Research Center, Cleveland, OH, 1967.

[25]Charles K Birdsall. Particle-in-cell charged-particle simulations, plus monte carlo collisions with neutral atoms, pic-mcc. *IEEE Transactions on Plasma Science*, 19(2):65–85, 1991.

[26]Charles K Birdsall and A Bruce Langdon. *Plasma physics via computer simulation*. CRC Press, 2004.

[27]Dmytro Sydorenko. *Particle-in-cell simulations of electron dynamics in low pressure discharges with magnetic fields*. PhD thesis, University of Saskatchewan Saskatoon, 2006.

[28]Vahid Vahedi and Maheswaran Surendra. A monte carlo collision model for the particle-in-cell method: applications to argon and oxygen discharges. *Computer Physics Communications*, 87(1):179–198, 1995.

[29]AV Phelps. The application of scattering cross sections to ion flux models in discharge sheaths. *Journal of applied physics*, 76(2):747–753, 1994. Phelps database, www.lxcat.net, retrieved on March 10, 2015.

[30]D Piscitelli, AV Phelps, J de Urquijo, E Basurto, and LC Pitchford. Ion mobilities in xe/ne and other rare-gas mixtures. *Physical Review E*, 68(4):046408, 2003. Phelps database, www.lxcat.net, retrieved on March 10, 2015.

[31]Leanne C Pitchford. *Swarm studies and inelasitc electron-molecule collisions: proceedings of the meeting of the Fourth International Swarm Seminar and the Inelastic Electron-Molecule Collisions Symposium*. Springer Verlag, 1987. Hayashi database, www.lxcat.net, retrieved on February 24, 2015.

[32]F.F. Chen. *Introduction to Plasma Physics and Controlled Fusion*, volume 1. Plenum Press, New York, 1984.

[33]M.D. West, C. Charles, and R.W. Boswell. Testing a helicon double layer thruster immersed in a space-simulation chamber. *Journal of Propulsion and Power*, 24(1):134–141, 2008.